

# Exploiting Low-Cost Directional Antennas in 2.4 GHz IEEE 802.15.4 Wireless Sensor Networks

Gianni Giorgetti <sup>#\*1</sup>, Alessandro Cidronali <sup>#2</sup>, Sandeep K.S. Gupta <sup>\*3</sup>, Gianfranco Manes <sup>#4</sup>

<sup>#</sup>*Department of Electronics and Telecommunications, Università degli Studi di Firenze  
Via di S. Marta 3, 50139 - Firenze, ITALY*

<sup>1</sup>gianni.giorgetti@unifi.it

<sup>2</sup>alessandro.cidronali@unifi.it

<sup>4</sup>gianfranco.manes@unifi.it

<sup>\*</sup>*School of Computing and Informatics, Arizona State University  
699 South Mill Avenue, Tempe AZ 85281, USA*

<sup>3</sup>sandeep.gupta@asu.edu

**Abstract**—Motivated by recent interest in directional antennas for WSNs, we propose a *Four-Beam Patch Antenna (FBPA)* designed to meet the size, cost and complexity constraints of sensor nodes. We use in-field experiments with COTS motes to demonstrate substantial benefits to WSN applications. Used outdoors, the FBPA extends the communication range from 140m to more than 350m, while indoors it suppresses the interference due to multipath fading by reducing the signal variability of more than 70%. We also show interference suppression from IEEE 802.11g systems and discuss the use of the antenna as a form of angular diversity useful to cope with the variability of the radio signal. Experimental data are analyzed to derive model parameters intended for use in future network simulations.

**Index Terms**—Wireless Sensor Networks, Directive Antenna, System Level Analysis.

## I. INTRODUCTION

The Wireless Sensor Network (WSN) [1] is a flexible and scalable paradigm that is drawing increasing attention due to its potential utilization in many civilian and military domains. Designed to work without infrastructures, WSNs exploit inexpensive sensor nodes and multi-hop radio communication to achieve large-scale coverage and high spatial resolution with limited costs. Such benefits have recently been demonstrated by many real world applications. One such example is the pilot site implemented at the University of Florence within the EU-IST GoodFood project [2], where a WSN is used to monitor vineyard physical and chemical targets relevant to plant physiologists. Long-term operations in the pilot site have shown that improving the efficiency of wireless communication is a key point to increase the reliability of a WSN. This is especially true in sparse networks, where the presence of a few unreliable radio links can determine loss of connectivity of a large number of sensors. In addition, since nodes are battery operated and wireless communication dominates the energy costs, ensuring a low error rate and rejection to multipath interferences avoids unnecessary retransmissions and thus increases the network lifetime.

While the directional antenna is an established technology that has been proven effective in improving the radio link quality, their use in WSN has not been explored until recently [3]-[4], mainly because of the cost and size constraints of

sensor nodes. Nevertheless, as radio communications move to higher frequencies and antenna dimensions shrink, integrating such technology on sensor nodes appears not only feasible, but also desirable to compensate for the higher path loss intrinsic of shorter wavelengths, to ensure higher link quality and to implement a form of antenna diversity.

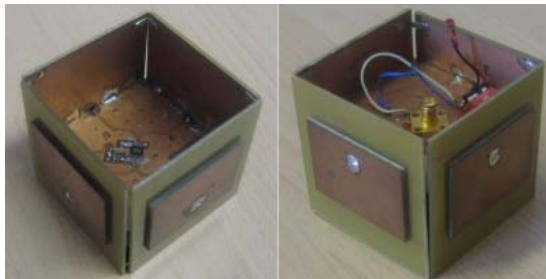


Fig. 1. Two views of the four-beam patch antenna

In light of the above considerations, we propose a switched beam directional antenna that satisfies the size, cost and complexity constraints typical of a sensor node. The antenna, designed for operations in the 2.4GHz ISM band (e.g. using the IEEE 802.15.4 standard), has dimensions comparable to those of commercially available sensor nodes (it can actually be used to shelter the node itself), has a simple design and implements the beam selection through two digital lines. After a brief description of the design principles provided in section II, we use in-field experiments and theoretical fading models to characterize the mote-to-mote link in different environments. The results are presented in section III, showing a considerable increment in the link budget and reduction of the signal variability respect to the omnidirectional radio link. In section IV, we consider the effect of interferences from IEEE 802.11g devices operating in the same 2.4GHz band and demonstrate interference suppression with improvement in the link quality and packet delivery ratio. Finally, in section V we show that the faces of the antenna implement a form of angular diversity, allowing the node to cope with radio interferences and avoid deep fade nulls caused by multipath reflections.

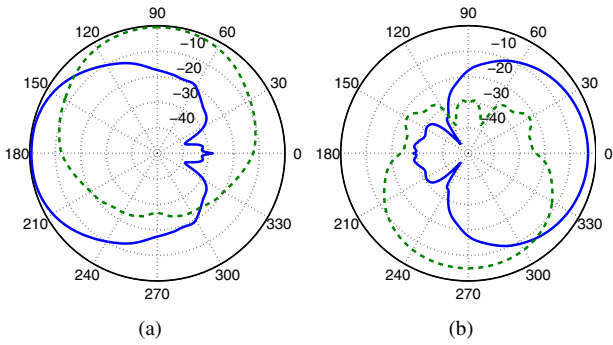


Fig. 2. Radiation pattern of the four antenna faces. a) Patch 1 (solid) & Patch 2 (dashed); b) Patch 3 (solid) & Patch 4 (dashed).

## II. FOUR-BEAM PATCH ANTENNA

The proposed *Four-Beam Patch Antenna* (FBPA) is composed of four coaxially fed planar patch antennas arranged in a “box like” structure as shown in fig. 1. Each face is realized on a two-layer RF4 substrate [5] having planar dimension of  $56\text{mm} \times 56\text{mm}$  and thickness of 2.4mm. The four patches, which operate in linear polarization, share a common design that has been optimized by using the Ansoft-HFSS CAD [6] to work in the 2.4 GHz ISM band. The mechanical arrangement of the four patches and their coaxial feeding is such that the vertical axis of the box coincides with the intersection of the E-planes of the single patches.

The RF signal is distributed to the four faces by a single-pole four-trough switch, which is controlled by two digital lines and allows the wireless node to dynamically select which face to use (c.f. section V). The loss due to the switch, the distribution networks and the mismatches are compressively evaluated in about 1.5 dB within the selected ISM band.

The characterization in the anechoic chamber has given the patterns reported in the fig. 2. In spite of the low-cost substrate, the patches gain measured to the external SMA connector, hence including the losses listed before, are comprised between 8.3dBi and 7.5dBi. From fig. 2 it is observed that the combined patterns ensure a uniform coverage of the 360 degree horizon.

## III. LINK QUALITY EXPERIMENTS

In this section we begin the characterization of the proposed antenna with a series of in-field experiments based on commercially available WSN nodes. The unit chosen for our tests is the TelosB platform [7], a low-power sensor board equipped with the Chipcon CC2420 radio module [8]. The transceiver operates in the 2.4 GHz band using O-QPSK modulation with *Direct Sequence Spread Spectrum* (DSSS) coding, which provides a process gain (PG) of 9 dB. The CC2420 achieves a maximum data rate of 250Kbps, -94 dBm of sensitivity, and it is compatible with the PHY and MAC layers defined by the new IEEE 802.15.4 standard. The omnidirectional (OD) antenna integrated on the TelosB board, an Inverted-F microstrip antenna [7], has been used as baseline for our tests.

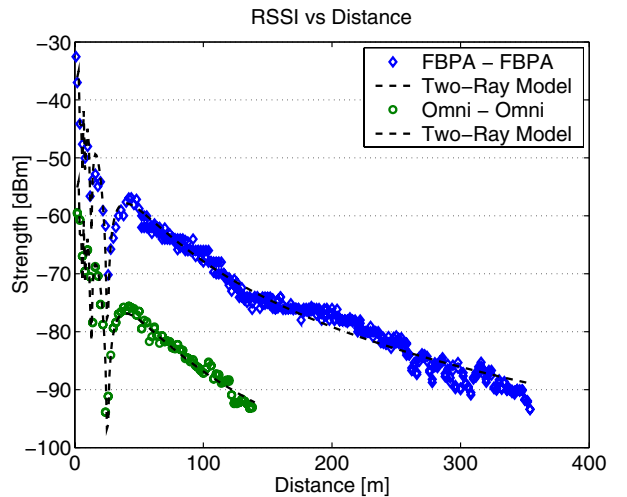


Fig. 3. Received signal strength as function of the distance. Transmission power is 0 dBm; values are averaged over 200 radio packets.

### A. Large-Scale Fading

In the first set of experiments we measured the *Received Signal Strength Index* (RSSI)<sup>1</sup> as a function of the nodes distance. The sensors, placed in an open space free of obstacles at 1.3 m above the ground, were set to transmit at 0 dBm (the maximum power allowed by the transceiver) and oriented with the active patches pointing toward each other. Figure 3 reports the RSSI measures averaged over 200 radio packets along with the signal strength computed using the Two-Ray large-scale fading model [9]. The model defines the value of the E-field  $E_{TOT}(d)$  at distance  $d$  taking into account the interference of the signal reflected from the ground:

$$|E_{TOT}(d)| = \frac{E_0 d_0}{d} \sqrt{2 - 2 \cos \theta_{\Delta}}, \quad (1)$$

where  $E_0$  is value of the E-field at distance  $d_0$  derived from the Friis free space equation. The value  $\theta_{\Delta}$  describes the phase shift due to the increased path length of the reflected signal. According to the model and the measures, for large distances the signal strength decays as a function of  $d^4$ , therefore the increased link budget (+20dB respect to the OD configuration) extends the maximum communication range from 140 m to over 350 m. The range measurements suggest that the proposed antenna is suitable for WSNs deployed over large areas where, without increasing the TX power, multiple OD radio hops can be replaced by few directional links. We observe that reducing the total number of hops not only decreases the transmission delay and the probability of error, but also has a considerable impact on the energy conservation within the network since it decreases the total number of transmissions and receptions.

<sup>1</sup>The CC2420 automatically generates 8-bit RSSI values upon reception of correct radio packets.

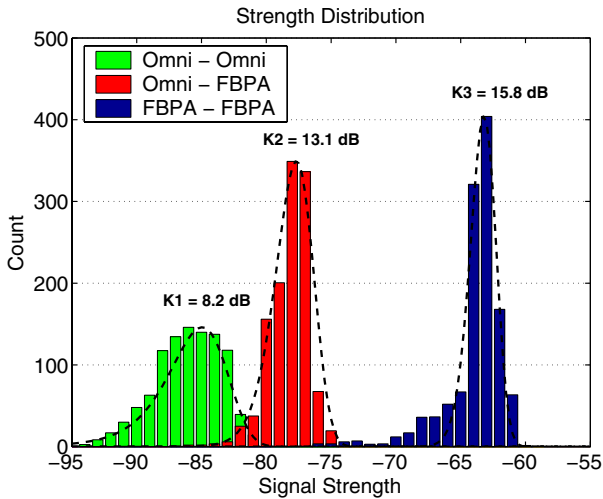


Fig. 4. Distribution of the received signal strength for three configurations: omni-omni (K1), omni-FBPA (K2), FBPA-FBPA (K3).

### B. Small-Scale Fading

The strength tests have been repeated indoors to characterize the effect of multipath interferences due to the presence of reflecting surfaces and people moving in proximity of sensor nodes. In figure 4, we report the distribution of the received signal strength for the case where the FBPA is first used on the receiver and then on both sides of the radio link. The histograms are compared to the Ricean distributions, a statistical model used to describe small-scale fading channels [9]. The Ricean distributions defines the probability of receiving a signal with amplitude of  $v$  volts, ( $v \geq 0$ ) as:

$$p(v) = \frac{v}{\sigma^2} e^{-\frac{(v^2+A^2)}{2\sigma^2}} I_0\left(\frac{Av}{\sigma^2}\right), \quad (2)$$

where  $I_0$  is the modified Bessel function of the first kind and zero order,  $A$  is the peak amplitude of the *line of sight* (LOS) component and  $\sigma^2$  is the time-average power of the received radio signal. The distribution is described by the parameter  $K = A^2/2\sigma^2$ , whose values are reported in fig. 4.

The use of the FBPA increases the  $K$  factor from 8.2 dB to 15.8 dB, demonstrating a substantial increment of the LOS component and reduction of the multipath interferences. In our experiment, the mean of the signal strength is increased by more than 22dBm using two FBPAs, while the variance is reduced by over 70% when there are one or two FBPAs.

## IV. REJECTION TO 802.11 INTERFERENCES

In a WSN the information gathered by the sensors is usually collected by a sink node and then forwarded to a gateway (e.g. a PC with an Internet connection) that dispatches the data to the remote users. In this section we consider the case where the gateway uses an IEEE 802.11g link that might interfere<sup>2</sup> with the packets received by the sink node. In our setup, the 802.11g source was located at 1.5 meters from the sink node,

<sup>2</sup>In our experiment the synch node uses the 802.15.4 Ch.17, while the 802.11g device operates on the overlapping band of Ch.6.

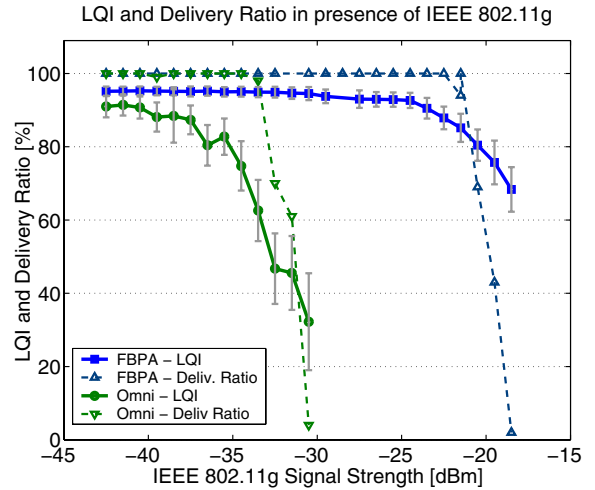


Fig. 5. LQI and Delivery Ratio as a function of the 802.11 interference power.

forming a 90 degree angle with the axis of the face used for reception (patch 3, see Fig. 2). The packets were transmitted by a FBPA node located at 5m from the sync node and set to -25dBm of power. Figure 5 reports the effect of the interference on the delivery ratio and the Link Quality Index (LQI)<sup>3</sup>. When the sync node uses an OD antenna, the delivery ratio and the LQI drops rapidly as the 802.11g interference source transmits above a value of -33 dBm. In the case of a node with directional antenna, the FBPA attenuates the interferences of about 14 dB and the quality of the link is not substantially affected until the 802.11g interference reaches the power of -19 dBm. The results can be explained with the fact that the error probability is proportional to the interference strength at the receiver input,  $P_I$ :

$$P_I = K \cdot P_{TX}^i \cdot L_p(d) \cdot G(\theta) \quad (3)$$

where  $P_{TX}^i$  is the power of the 802.11g source,  $L_p(d)$  is the path loss as function of the distance  $d$  and  $G(\theta)$  is the directional gain of the antenna in the direction of the emission source. Finally,  $K$  is a factor that accounts for the portion of IEEE 802.11g power that falls in the 802.15.4 channel (approximately 19%) [10]. Having fixed the distance  $d$  and the angle  $\theta$ , the link quality is solely affected by the interference power  $P_{TX}^i$ . In our experiments, the angle  $\theta$  was equals to 90 degrees with respect to the active face (patch 3) and the increased immunity to the interference can be justified by the reduced gain of the antenna in that direction. Although the experiment was conducted in the lab using small power levels and short distances, the values can be easily scaled to determine how the sink node should be positioned with respect to the 802.11g source to avoid interferences in a real-case scenario.

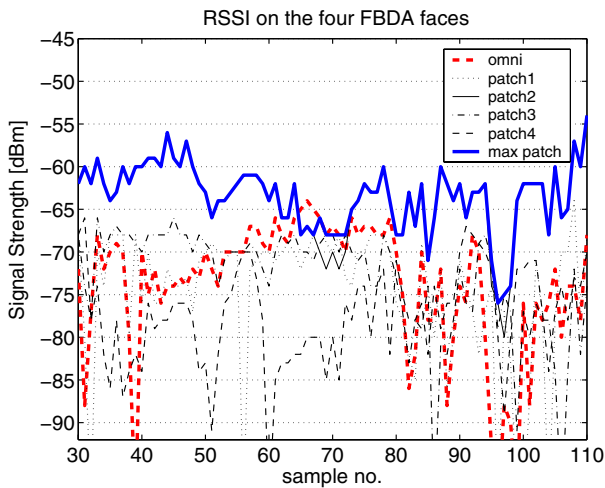


Fig. 6. Samples of signal strength measured on the four antenna patches.

## V. ANGULAR DIVERSITY

In a typical WSN application each sensor exchanges information with other nodes located at different positions, therefore a switching policy is needed to determine the patch to be used for each communication. If the network is static and node positions are known, these data can be preloaded into each unit and the selection can be implemented by using the face pointing in the direction of the other node. Anyway, in the general case positions are not known in advance (ad hoc deployment) or the face pointing toward the other node might not be the best selection due to the presence of multipath, reflections and scattering of the signal. In these cases the best patch can be dynamically determined during the setup phase of the network by exchanging a few radio beacons with the surrounding nodes and selecting the face that ensures better signal strength. While the antenna selection problem has been addressed in relation to MAC and routing protocols for ad-hoc WSNs [3]-[11], we note that by allowing a node to dynamically switch among different beams, the directive antenna implements a form of angular diversity that increases the reliability of communication [12]. This is especially important when nodes are static and the presence of a deep fade null can affect the communication for an indefinite period of time. Using the four faces of the FBPA, the node is given the opportunity to choose among four low correlated radio channels, thus increasing the probability of successful communication. In the last experiments a node with the directive antenna is used to communicate with an OD node that is moved through different positions. Fig. 6 compares the signal strength received at the four patches with the signal received by an OD antenna placed at the same position.

<sup>3</sup>The LQI is a metric defined by the IEEE 802.15.4 that measures the error in the incoming modulation and provides an estimation of the expected delivery ratio on a given radio link.

While all of the lines fluctuate and have deep fades, the ability to select the face with maximum RSSI ensures stable receptions. In our experiment, the correlation coefficient for the strength values received by different faces was comprised from a max of 0.43 for face 1 and 2, to a min of 0.15 for face 1 and 3.

## VI. CONCLUSION

The Four-Beam Patch Antenna has been proposed as a solution to improve radio communication in WSNs. Specifically, we showed that the FBPA is effective in increasing the radio range by more than 100m, decreasing the variance of the signal by about 70% and suppressing in-band interferences. The above benefits are achieved with a low-cost and small-size solution that meets the constraints typical of WSN applications. In addition, the correspondence between experimental data and theoretical models is examined to derive the system parameters that we plan to use for network simulations and future research in the field of directional antennas for WSNs.

## ACKNOWLEDGMENT

The authors wish to thank R. Nesti for his assistance during the antenna pattern measurements, S. Maurri for the prototype fabrication, E. Raleigh and A. Giorgetti for their help during the in-field experiments and L. Sparbel, G. Collodi, D. Di Palma and A. Manes for their helpful suggestions.

## REFERENCES

- [1] I. F. Akyildiz, W. Su, Y. Sankarasubramaniam, and E. Cayirci, "Wireless sensor networks: a survey," *Computer Networks*, vol. 38, no. 4, pp. 393–422, 2002.
- [2] The GoodFood European Project (FP6-IST-1-508744-IP), <http://www.goodfood-project.org>, 2004.
- [3] C. Santivanez and J. Redi, "On the use of directional antennas for sensor networks," in *MILCOM 2003*, vol. 1. IEEE, 2003, pp. 670–675.
- [4] D. Leang and A. Kalis, "Smart sensordvb: sensor network development boards with smart antennas," in *International Conference on Communications, Circuits and Systems*, vol. 2, 2004, p. 1476–1480.
- [5] C. A. Balanis, *Antenna theory analysis and design*. New York: J. Wiley and Sons, 1997.
- [6] Ansoft, "HFSS," <http://www.ansoft.com/products/hf/hfss/>.
- [7] Moteiv Corporation, "Telos (rev b) datasheet," <http://www.moteiv.com>, 2004.
- [8] Chipcon, "Chipcon cc2420 datasheet," [http://www.chipcon.com/files/CC2420\\_Data\\_Sheet\\_1\\_4.pdf](http://www.chipcon.com/files/CC2420_Data_Sheet_1_4.pdf).
- [9] T. S. Rappaport, *Wireless Communications: Principles and Practice*, 2nd ed. pub-PHPTR:adr: P T R Prentice-Hall, 2002.
- [10] S. Y. Shin, S. Choi, H. S. Park, and W. H. Kwon, "Lpacket error rate analysis of IEEE 802.15.4 under IEEE 802.11b interference," in *WWIC*, 2005, pp. 279–288.
- [11] T. Dimitriou and A. Kalis, "Efficient delivery of information in sensor networks using smart antennas," pp. 109–122, 2004.
- [12] C.-L. Yang, J. Mastarone, and W. Chappell, "Directional antennas for angular diversity in wireless sensor networks," in *Antennas and Propagation Society International Symposium*, vol. 4A. IEEE, 2005, pp. 263–266.